APPLICATION OF A PYRAMIDAL IMAGE MATCHING SCHEME FOR SHORT-TERM CLOUD AND IRRADIANCE PREDICTION IN THE HAWAIIAN ISLANDS

Steven H. Young
John W. Zack
AWS Truepower
463 New Karner Road
Albany, NY 12205
steve@meso.com
jzack@awtruepower.com

ABSTRACT

Numerous techniques have been developed that use a sequence of satellite images to predict short-term cloud evolution and solar electricity generation. All use a single-scale approach to estimating cloud motion patterns that contain multiple scales of features. This paper addresses this shortcoming with a technique based on a pyramidal image-matcher (PIM).

The PIM averages images of clear-sky index (CSI - the ratio of irradiance to clear-sky irradiance) to N additional grids with spacing of 2, 4,… 2N times the native resolution. The PIM estimates a motion field from two consecutive images at the coarsest resolution. It refines the estimate by computing corrections at successively higher resolutions.

The cloud motion field estimate is applied to the most recent image to predict CSI patterns over the next 3 hours that are then used to predict the irradiance and solar electric power generation. The PIM has been applied to predict rooftop PV generation in Hawaii. Its performance is evaluated with ground-based measurements and visible satellite estimates of irradiance.

1. INTRODUCTION

The prediction of solar electrical generation in the 0 to 3 hour-ahead timeframe presents a unique challenge. Numerical Weather Prediction (NWP) models typically do not resolve the smaller-scale cloud features important at these time scales, or do not have access to sufficient observations to properly represent these features in their initial conditions. Persistence based methods typically have skill only in the sub-hourly time frame. Even in environments where sky conditions tend to be highly persistent such as Hawaii, the events that represent a change in sky conditions are of most interest to electric grid operators as these events require active management.

Numerous methods that predict cloud motion from two consecutive satellite images have been applied to this problem (1, 2). These methods match sub-regions of the two images using various statistical approaches. The two sub-regions that represent the best match are considered to be the beginning and ending of a trajectory that defines a cloud motion vector. They can successfully track cloud motions as well as growth and decay. They are limited in their prediction ability by 1) the lifetimes of the clouds which they track, 2) the rate of change of the cloud motion field and 3) by their ability to identify the different scales of motion that impact clouds and assemble them into a realistic cloud motion field. The Pyramidal Image Matcher (PIM) technique (3) has the advantage of identifying cloud motion fields at the largest scales and, by applying successive corrections at smaller and smaller scales, incorporating the smaller scales of motion into the cloud motion field.

This paper describes the use of the PIM technique in forecasting short-term cloud evolution in Hawaii. Section 2 describes the method. The initial experiment technique is described in section 3. Results are presented in section 4. A summary, conclusions and direction of future work are presented in section 5.

2. METHOD

The initial version of the PIM technique (3) for the Hawaiian application accepts as input 2 km resolution images of CSI over a grid of 1120x1040 points centered on the Hawaiian Islands. Images are available every 15 minutes. CSI is derived from visible satellite images using

the techniques of Perez, et. al. (2) which was built upon earlier work by (5, 6). Atmospheric turbidity values were assigned based on (7, 8).

The PIM then uses the 2 most recent images, image A (the older image valid at time t_A), and image B (the most recent image valid at time t_B) to estimate the cloud motion field. If a gap between images of greater than 30 minutes is present, the estimation is not performed. The estimation is performed in the following steps:

1. Images are averaged to N additional grids with spacing of 2, 4,… 2N times the native resolution. In this case, the resolutions are 4, 8 and 16 km.
2. The cloud motion field is estimated at the 16 km resolution at each grid point (i, j) as follows:
    a. The 49 grid points that form a 7x7 square centered on point (i, j) in image B are selected. This set of grid points is defined as the central cluster)
    b. A set of clusters identical in size and shape to the central cluster are selected from image A centered on the 25 grid points extending from (i-2, j-2) to i+2,j+2). These clusters are known as displaced clusters. In this case, the maximum displacement is 2 grid points in each direction.
    c. A weighted mean squared difference between the CSI at each of the 49 points in the central cluster and the CSI at corresponding points in each displaced cluster is computed using a Gaussian weighting that assigns higher weights to the points nearer to the center of the cluster.
    d. The motion vector is defined as beginning at the center of the displaced cluster with the smallest mean squared difference and ending at the central cluster. Figure 1 shows a schematic of a sample computation.
3. Once the cloud motion field, V is computed at every grid point, it is smoothed and interpolated to the full 2-km resolution.
4. The motion field is applied to image A to predict the CSI at time t_B. The resulting image is known as image B`.
5. Image B` is averaged to the next finer resolution (8 km).
6. Images B and B`, both at 8-km resolution are then used to compute a correction to V, denoted as V`. This is done by repeating steps 2-3.
7. V' is then added to V to produce a corrected motion field.
8. Steps 5 through 7 are repeated, this time averaging to 4 km.
9. The correction process is repeated until the full resolution is reached and V represents motion at all scales from 16 to 2 km.

Once the final correction is added to V, it is applied to image B at full resolution to compute the predicted image 15-minutes in the future. The motion field is then applied to the 15-miute forecast to generate a 30-minute forecast. This is repeated until the end of the forecast period is reached.

The value of N, the cluster dimensions, maximum displacement, sharpness of the Gaussian weighting function and degree of vector field smoothing are adjustable parameters in this technique.

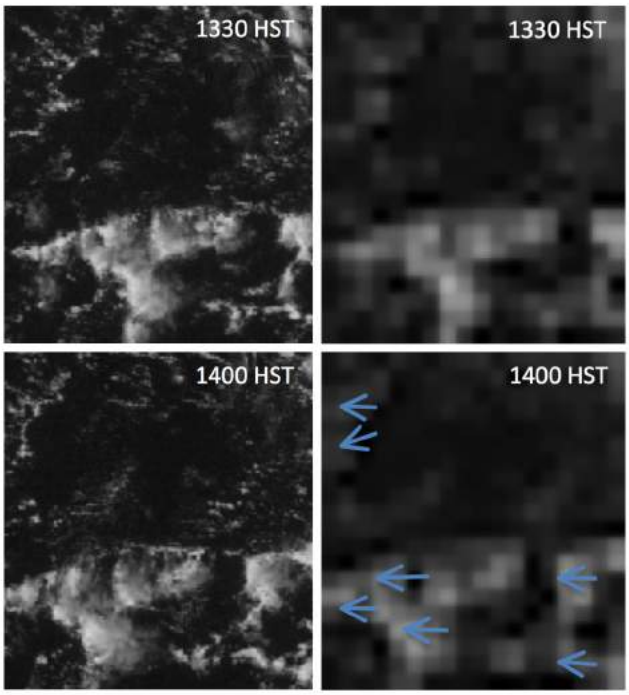

Fig. 1: 1 km (left) and 8 km (right) resolution images northeast of Oahu, Hawaii at 1330 HST (top) and 1400 HST (bottom). The blue vectors on the bottom right image show sample motion vectors computed at 8 km resolution from those cloud features that are resolvable at this resolution.

3. EXPERIMENT

As of this writing, a forecasting experiment over Hawaii was in progress. At this time, gridded forecasts of CSI were generated at 15-minute intervals out to a look-ahead time of 2 hours. Forecasts were generated at all times for which a visible satellite image was available at forecast time and a second image was available either 15 or 30 minutes before the forecast time from the period of 12 December 2012

through 11 February 2013 for the Hawaiian Islands and surrounding ocean. Verification results are available as averaged mean absolute error (MAE) of CSI over sub-grid regions that include Oahu, the island group of Maui, Molokai and Lanai, and the Big Island. Figure 2 shows the verification regions.

Forecasts will continue to be generated in real time. Updated results will be presented at the conference. This will include 3-hour forecasts through 31 March 2013, verification at ground based measurement sites and experiments with PIM user adjustable parameters.

Fig. 2: Verification regions for the PIM forecast technique including Oahu (upper left), the Big Island (upper right) and Maui, Molokai and Lanai (bottom).

4. RESULTS.

Figure 3 shows the MAE of the PIM forecasts and a persistence forecasts over about 700 forecasts from 12 December 2012, through 11 February 2013 for regions of the forecast grid that include: A) Oahu and the surrounding ocean, B) Maui, Molokai, Lanai and surrounding ocean and C) Big Island and surrounding ocean. The PIM errors are about 5-10% less than those for persistence. The performance vs. persistence improves significantly with increasing forecast look-ahead time for Oahu, and slightly with time for Maui, Molokai and Lanai. Performance vs. persistence decreases slightly with forecast look-ahead time for Big Island.

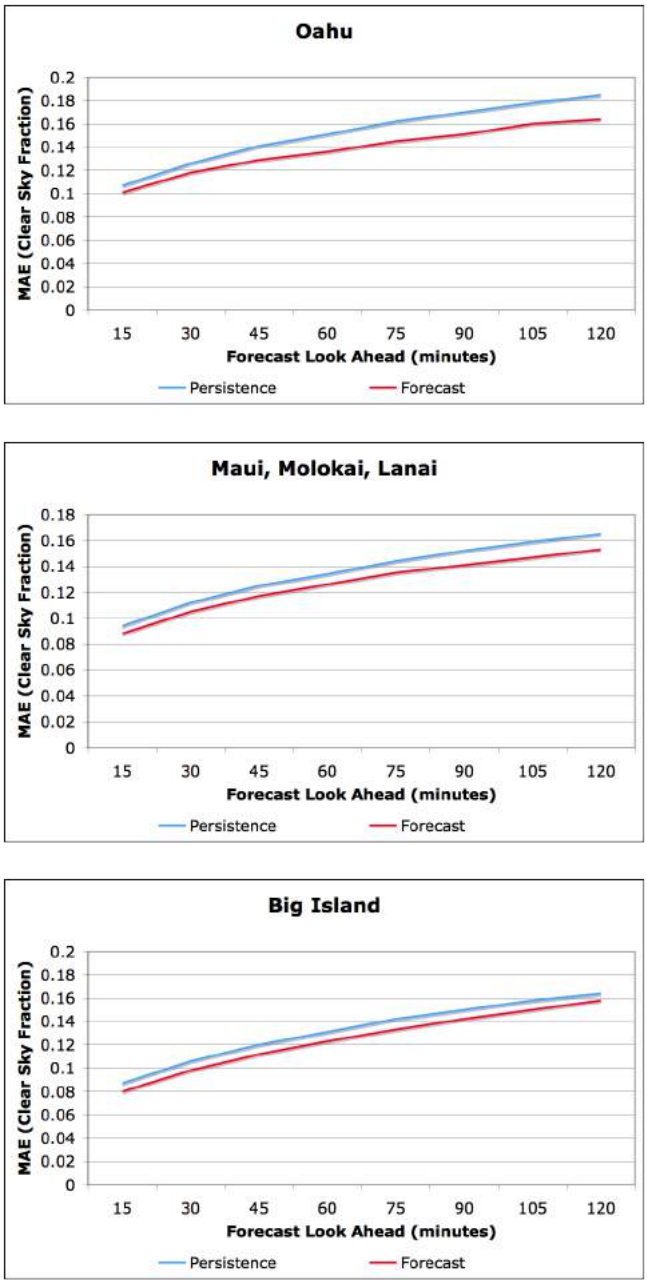

Fig. 3: Mean absolute forecast error of clear-sky index for a persistence based technique and the pyramidal image-matcher for (top) Oahu and surrounding ocean; (middle) Maui, Molokai and Lanai and surrounding ocean; and (bottom) Big Island and surrounding ocean for approximately 700 forecasts issued between 11 December 2012 and 11 February 2013.

Figure 4 shows the performance of the one-hour forecast vs. the hour of the day in which the forecast verified over the same regions. Figure 4 shows that error is largest early in the day when the sun is low in the sky and it is more difficult to determine the clear sky index from visible satellite imagery. It also shows that the pyramidal image matcher has an advantage over persistence mainly in the afternoon, especially the late afternoon. The one exception is Big Island where a small advantage persists through most of the day.

Error statistics are now being computed at all sites with a surface irradiance observation. However, cumulative results have not yet been compiled for these sites. In addition, software is being developed to compile and map error statistics by grid point.

5. SUMMARY, DISCUSSION AND CONCLUSION

A short-term solar forecasting method was developed based on applying a pyramidal image matcher to recent satellite images. The method was applied to the 0-2 hour forecast of Clear Sky Index (CSI) on the islands of Oahu, Molokai, Lanai, Maui and the Big Island in the state of Hawaii. Initial results show that the MAE of the CSI forecast is 5-10% better than a persistence-based forecast.

Forecasting using satellite-based methods is difficult in Hawaii since cloud features over land tend to be fixed to the terrain. These features tend to develop and dissipate over a somewhat regular diurnal cycle. Meanwhile, cloud features over water tend to move with the prevailing easterly trade wind flow. The information provided by two successive satellite images may not be sufficient to distinguish between these two different types of cloud evolution. Furthermore, the technique is able to predict neither changes in the net growth or decay of cloud features nor the tendency of clouds anchored in the trade wind flow to slow, grow or otherwise change their motion as they approach an island. These two limitations are particularly challenging for forecasts beyond a time horizon of about an hour.

These forecasting challenges make verification against a persistence-based forecast particularly challenging given the highly persistent cloud distribution over the islands. One area of future work will attempt to address this issue by computing error statistics for times when the cloud pattern is not persistent.

Other areas of work will focus on verification of 3-hour forecasts through 31 March 2013, verification of irradiance forecasts at ground based measurement sites and testing the sensitivity of forecast performance to the values of the adjustable parameters in the PIM scheme.

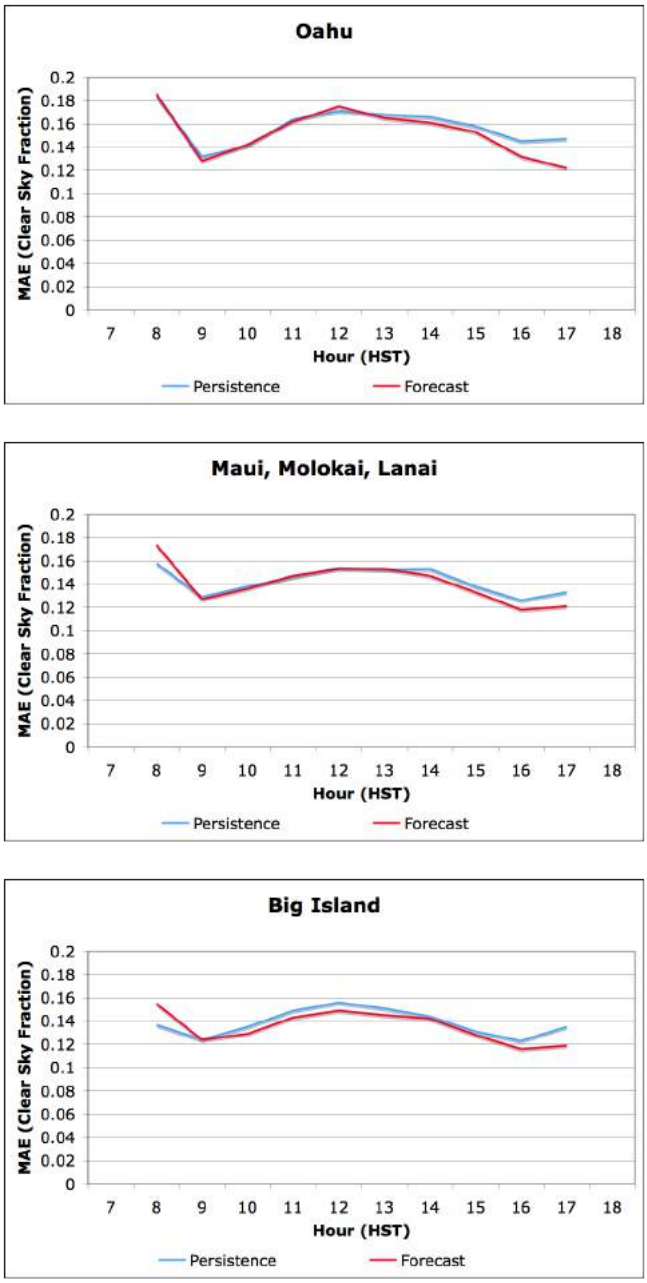

Fig. 4: Mean absolute forecast error of the 1-hour clear-sky index forecast vs. hour of the day for a persistence based technique and the pyramidal image-matcher for (top) Oahu and surrounding ocean; (center) Maui, Molokai and Lanai and surrounding ocean; and (bottom) Big Island and surrounding ocean for approximately 700 forecasts issued between 11 December 2012 and 11 February 2013.

6. ACKNOWLEDGEMENTS

The pyramidal image matcher cloud forecasting system was developed under a project funded through the Department of Energy and supported by the Hawaiian Electric Company, and through an Electric Power Research Institute sponsored project to develop solar forecasting services for Hawaii.

7. REFERENCES

(1) Hammer, D. Heinemann, E. Lorenz, B. Luckehe, Short-term forecasting of solar radiation: a statistical approach using satellite data, Solar Energy,(67):1–3, pp. 139–150, 1999.

(2) Hamill, T. M., and T. Nehrkorn, 1993: A short-term cloud forecast scheme using cross-correlations. *Wea. Forecasting*, 8, 401-411.

(3) Zinner, T., H. Mannstein, A. Tafferner, 2008: Cb-TRAM: Tracking and monitoring severe convection from onset over rapid development to mature phase using multi-channel Meteosat-8 SEVIRI data. Meteor. Atmos. Phys. 101, 191–210, DOI 10.1007/s00703-008-0290-y.

(4) Perez, R., P. Ineichen, K. Moore, M. Kmiecik, C. Chain, R. George and F. Vignola, 2002: A new operational model for satellite-derived irradiances: Description and validation. Solar Energy, 73, 307-317.

(5) Cano D., Monget J. M., Aubuisson M., Guillard H., Regas N. and Wald L.,1986: A method for the determination of global solar radiation from meteorological satellite data. Solar Energy, 37, 31–39.

(6) Zelenka A., Perez R., Seals R. and Renne´ D., 1999: Effective accuracy of satellite-derived irradiance. Theor. Appl. Climatol., 62, 199–207.

(7) Bason, F., 2008: Linke's turbidity factor applied to worldwide global horizontal irradiance measurements. http://www.soldata.dk/%5CPDF%5CPaper%20FB%20Lisbon%202008.pdf.

(8) Zelenka A., R. Perez, R. Seals and D. Renné,1999: Effective accuracy of satellite-derived irradiance. Theor. Appl. Climatol. 62, 199–207.